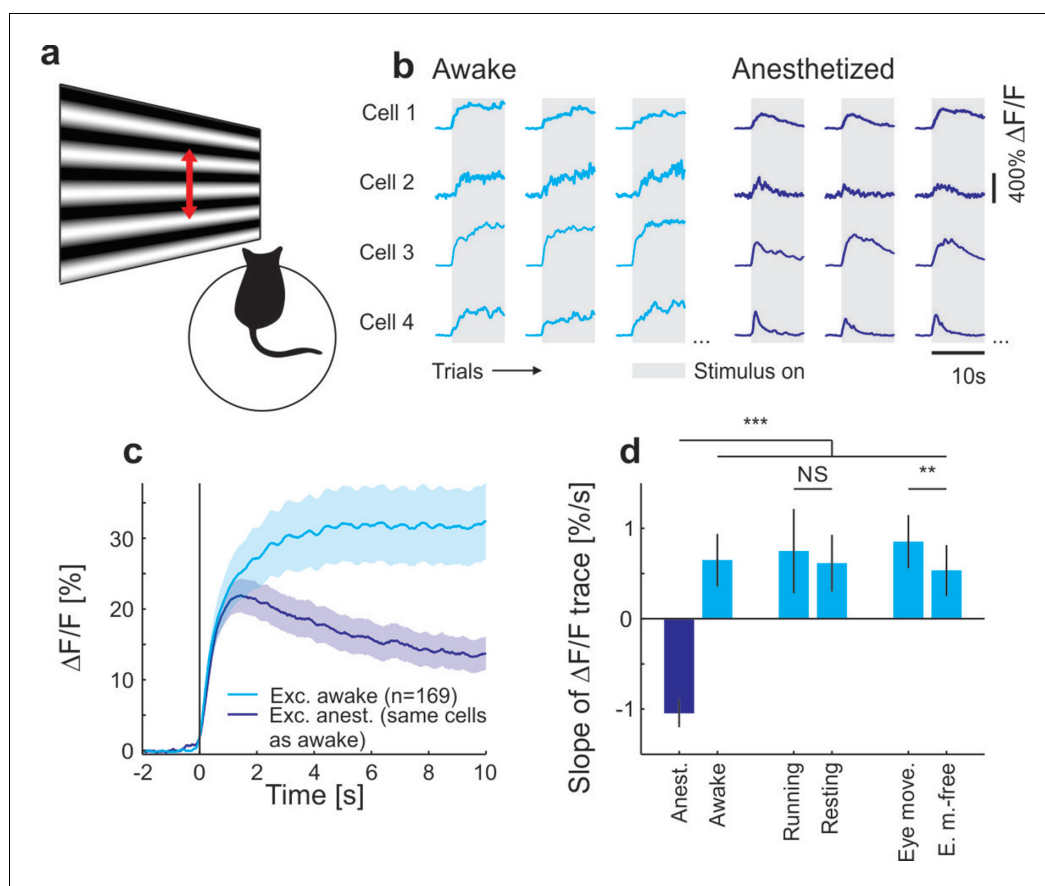


---

## Figures and figure supplements

Stimulus relevance modulates contrast adaptation in visual cortex

**Andreas J Keller et al**



**Figure 1.** Contrast adaptation in awake and anesthetized mice. (a) Schematic of the experimental setup. Calcium imaging with GCaMP6m (Chen et al., 2013) was performed during the presentation of drifting sinusoidal gratings. (b) Calcium transients from four example putative excitatory cells tuned to a moving sinusoidal grating at 50% contrast (presented for 10 s; grey shadings). The same cells were recorded during wakefulness and anesthesia. (c) Averaged calcium responses of tuned putative excitatory cells. Note that even small differences in adaptation can be detected using two-photon imaging (Figure 1—figure supplement 2a–d). Curves plotted as mean  $\pm$  SEM (shading). (d) Slope of adaptation of single cells recorded in different behavioral states (same data as in c; line fit to the data in time window 1–9.75 s). Anesthetized mice show a significantly more negative slope compared to all other states [anest. (169 cells) – awake (169 cells):  $p < 10^{-10}$ ; Wilcoxon signed-rank; running (51 cells):  $p < 10^{-4}$ ; resting (169 cells):  $p < 10^{-10}$ ; eye movements (168 cells):  $p < 10^{-10}$ ; eye movement-free (165 cells):  $p < 10^{-10}$ ; Wilcoxon rank-sum]. There was no significant difference between running and resting mice, as opposed to the significant but small difference in eye movement and eye movement-free trials ( $p = 0.49$  and  $p = 0.0047$ , respectively; Wilcoxon rank-sum). NS, not significant; \*\* $p < 0.005$ ; \*\*\* $p < 0.0005$ .

DOI: 10.7554/eLife.21589.002

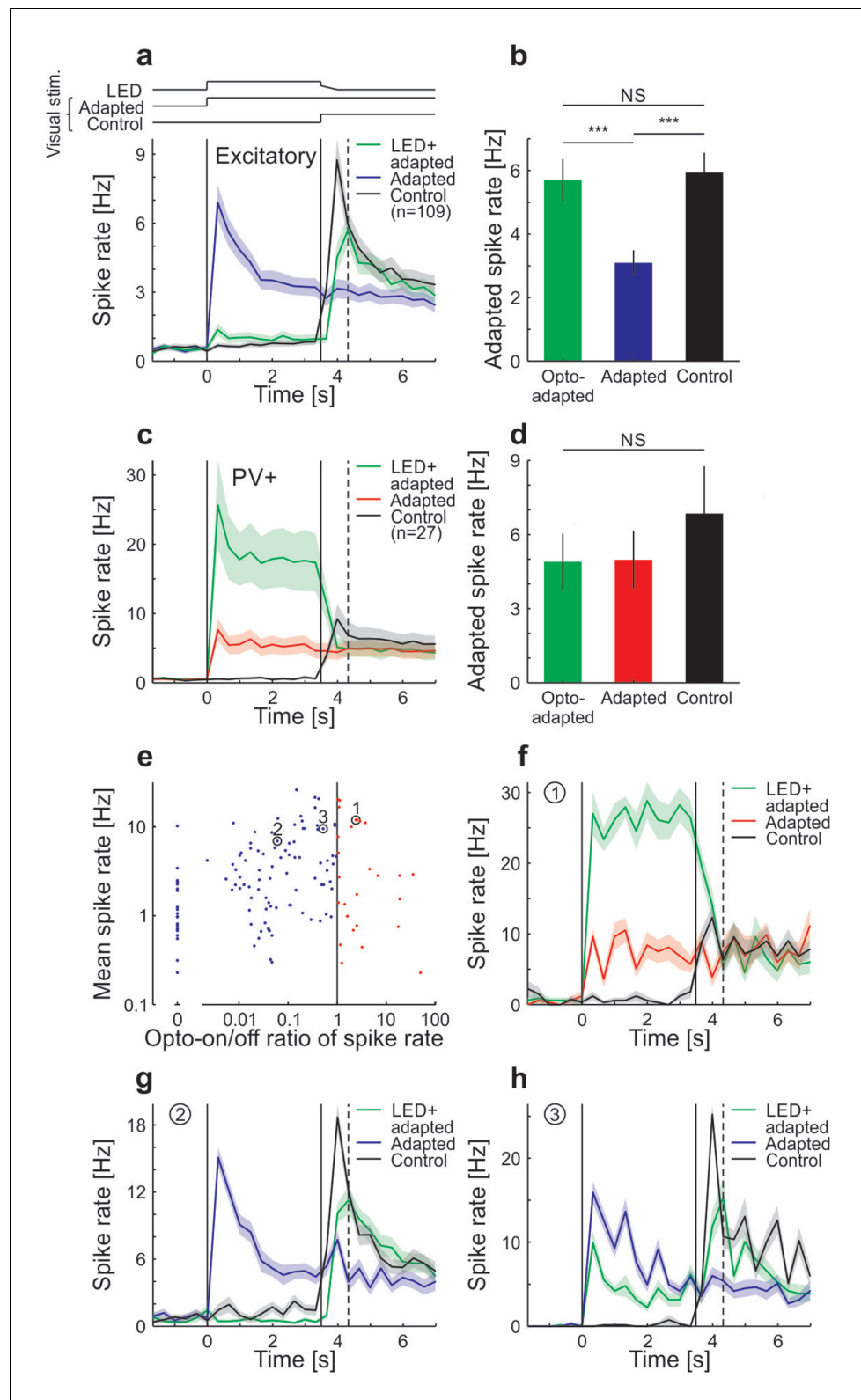


**Figure 1—figure supplement 1.** Adaptation in visual cortex of anesthetized mice is prevented by optogenetic silencing of cortical neurons (see also [King et al. 2016](#)). Neural activity was recorded with multi-tetrode arrays in anesthetized mice that express channelrhodopsin-2 (ChR2) in parvalbumin-positive (PV+) neurons. To test whether adaptation in V1 depends on local cortical activity, we presented a sustained moving grating with or without

*Figure 1—figure supplement 1 continued on next page*

*Figure 1—figure supplement 1 continued*

locally silencing the visual cortex and probed the V1 activity level immediately after the manipulation time window. (a) Averaged and binned (bin size 333 ms) spike responses of tuned putative excitatory cells to a moving square-wave grating at 100% contrast in anesthetized mice. The responses for three stimulus conditions are shown: Adapted, grating presented for 7 s; Control, grey screen presented for 3.5 s followed by 3.5 s of grating; LED + adapted, grating presented for 7 s with simultaneous optogenetic activation of PV+ cells during the first 3.5 s followed by a 0.5 s decrease of the optogenetic activation of PV+ cells (see Materials and methods). LED (optogenetic activation) and visual stimulus timings are illustrated by the top traces and marked by the vertical solid lines. The vertical dotted line indicates the time bin (first bin after LED off) used to compare the state of adaptation of the three stimulus conditions in b. Average traces are plotted as mean  $\pm$  SEM (shading). (b) Averaged spike rate for the three stimulus conditions for the bin indicated by the vertical dashed line in a. The LED+adapted condition evokes similar spike rates compared to the control and significantly more than the adapted condition (tuned putative excitatory: 109 cells; LED+adapted/adapted:  $p < 10^{-10}$ ; LED+adapted/control:  $p = 0.13$ ; adapted/control:  $p < 10^{-10}$ ; Wilcoxon signed-rank). Bars plotted as mean  $\pm$  SEM. (c) Same as a but for PV+ cells. (d) Same as b but for PV+ neurons. All conditions evoke similar spike rates (tuned PV+: 27 cells; LED + adapted/adapted:  $p = 0.73$ ; LED+adapted/control:  $p = 0.067$ ; adapted/control:  $p = 0.17$ ; Wilcoxon signed-rank). (e) Scatterplot of the average spike rate responses of all cells during the first 3.5 s of their preferred grating stimulus, with and without optogenetic stimulation of PV+ cells. Cells that increased their firing during the optogenetic stimulation of PV+ cells were classified as PV+ neurons, the remaining ones as putative excitatory cells. Highlighted cells (1–3) are shown in f–h. (f) Same as a but for a single cell classified as PV+. (g,h) Same as f but for two example cells classified as putative excitatory. NS, not significant; \*\*\* $p < 0.0005$ .

DOI: [10.7554/eLife.21589.003](https://doi.org/10.7554/eLife.21589.003)

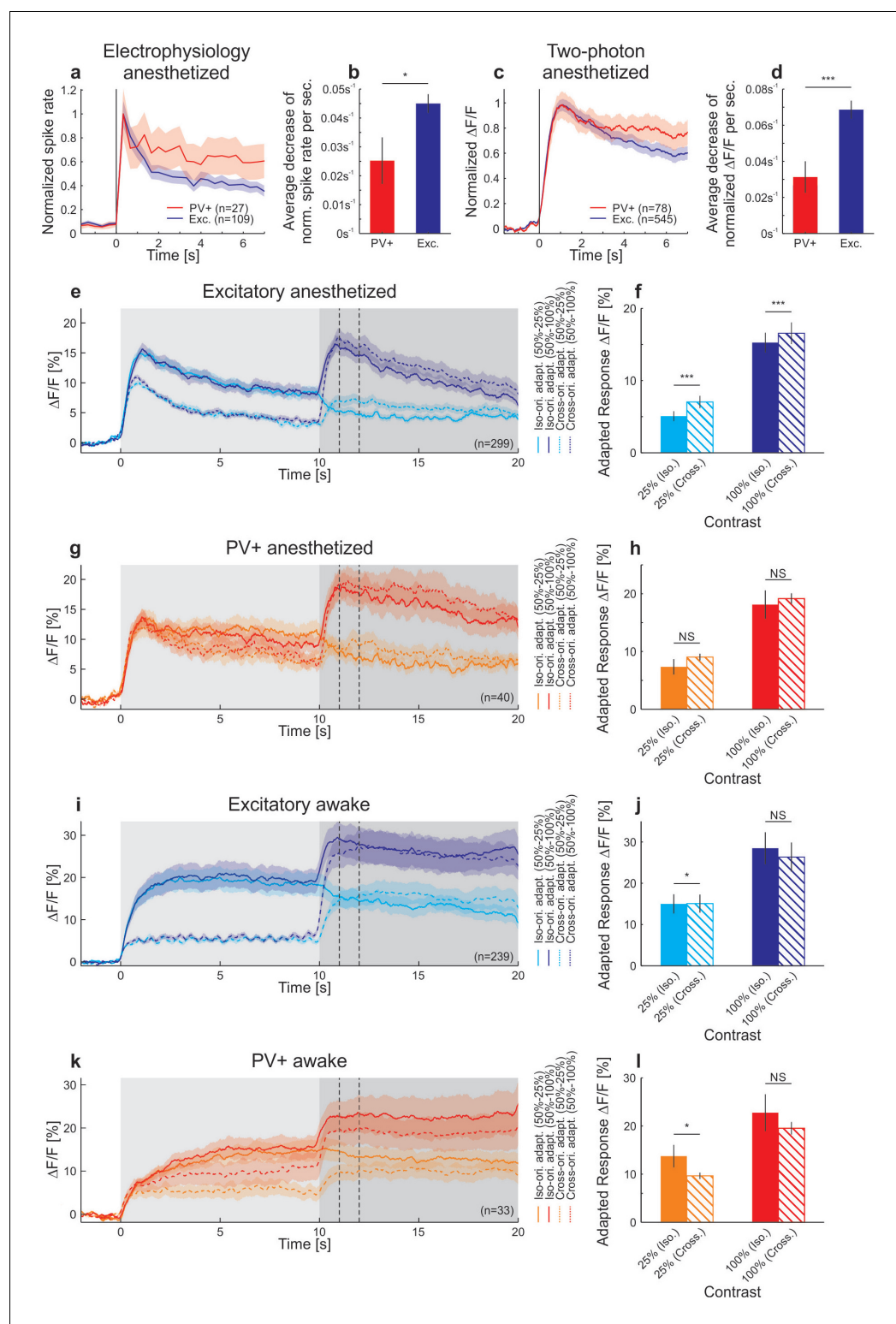


**Figure 1—figure supplement 2.** Differences in contrast adaptation across cell-types can be revealed using two-photon imaging. Under anesthesia, PV+ neurons adapted less than putative excitatory cells, consistent with the idea that they might inhibit other neurons to produce contrast adaptation (Keller and Martin, 2015). Moreover, iso- and cross-orientation adaptation had similar effects on the population (see also Stroud et al., 2012). In mouse V1, PV+ neurons are much less selective to a grating of different orientations than excitatory neurons (Atallah et al., 2012; Hofer et al., 2011; Kerlin et al., 2010). Therefore, an adaptation mechanism based on PV+ Figure 1—figure supplement 2 continued on next page

Figure 1—figure supplement 2 continued

neurons would result in adaptation that is only weakly dependent on the orientation of the stimulus. Indeed, adapting putative excitatory cells to their preferred or null (orthogonal to preferred) orientation results in a significant, but small difference in adapted firing rates. Moreover, no difference was found when adapting PV+ cells with either iso- or cross-orientation under anesthesia (with respect to test orientation). (a) Neural activity was recorded with multi-tetrode arrays in anesthetized mice (same cells as in **Figure 1—figure supplement 1a,b**). Averaged and normalized responses of tuned putative excitatory and PV+ cells to a moving square-wave grating at 100% contrast presented for 7 s in anesthetized mice. Curves plotted as mean  $\pm$  SEM (shading). (b) Adaptation is quantified as the mean decrease in the normalized spike rate per second during the stimulus presentation (tuned putative excitatory: 109 cells; PV+: 27 cells;  $p=0.010$ ; Wilcoxon rank-sum). Bars plotted as mean  $\pm$  SEM. (c) The neural activity of tuned putative excitatory compared to PV+ cells recorded with two-photon calcium imaging. Averaged and normalized calcium responses to a moving sinusoidal grating at 50% contrast presented for 7 s in anesthetized mice. Curves plotted as mean  $\pm$  SEM (shading). (d) Adaptation is quantified as the mean decrease in normalized  $\Delta F/F$  per second during the stimulus presentation (tuned putative excitatory: 545 cells; PV+: 78 cells;  $p=3.7 \times 10^{-4}$ ; Wilcoxon rank-sum). The initial rise was excluded in the estimation of the slope (see Materials and methods). (e) Averaged responses of tuned putative excitatory cells in anesthetized mice to a moving sinusoidal grating at 50% contrast presented for 10 s followed by 10 s of a second stimulus of increased (100% contrast; dark traces) or decreased contrast (25% contrast; light traces). The first stimulus was either presented at the optimal (solid traces) or the orthogonal orientation of the neurons (dotted traces). The second stimulus was always presented at the optimal orientation. The two vertical dotted lines indicate the time window which was used to compare iso- and cross-orientation adaptation in f.  $\Delta F/F$  traces plotted as mean  $\pm$  SEM (shading). (f) Iso-orientation compared to cross-orientation adaptation (50% contrast) of tuned putative excitatory cells measured at 25% or 100% contrast. This is quantified as average  $\Delta F/F$  after adaptation (seconds 11–12; indicated by the vertical dotted lines in e; 299 cells; 25%:  $p < 10^{-10}$ ; 100%:  $p < 10^{-4}$ ; Wilcoxon signed-rank). (g) Same as e but for PV+ cells. (h) Same as f but for PV+ cells (40 cells; 25%:  $p=0.12$ ; 100%:  $p=0.98$ ; Wilcoxon signed-rank). (i) Same as e but in awake mice. Note that the absence of adaptation to the moving sinusoidal grating at 50% contrast (0–10 s) cannot be explained by a response ceiling since the cells increase their responses when increasing the contrast to 100% (at 10 s). (j) Same as f but in awake mice (239 cells; 25%:  $p=0.0082$ ; 100%:  $p=0.14$ ; Wilcoxon signed-rank). (k) Same as i but for PV+ cells. (l) Same as j but for PV+ cells (33 cells; 25%:  $p=0.0064$ ; 100%:  $p=0.20$ ; Wilcoxon signed-rank). Bars plotted as mean  $\pm$  SEM. NS, not significant; \* $p < 0.05$ ; \*\*\* $p < 0.0005$ .

DOI: [10.7554/eLife.21589.004](https://doi.org/10.7554/eLife.21589.004)

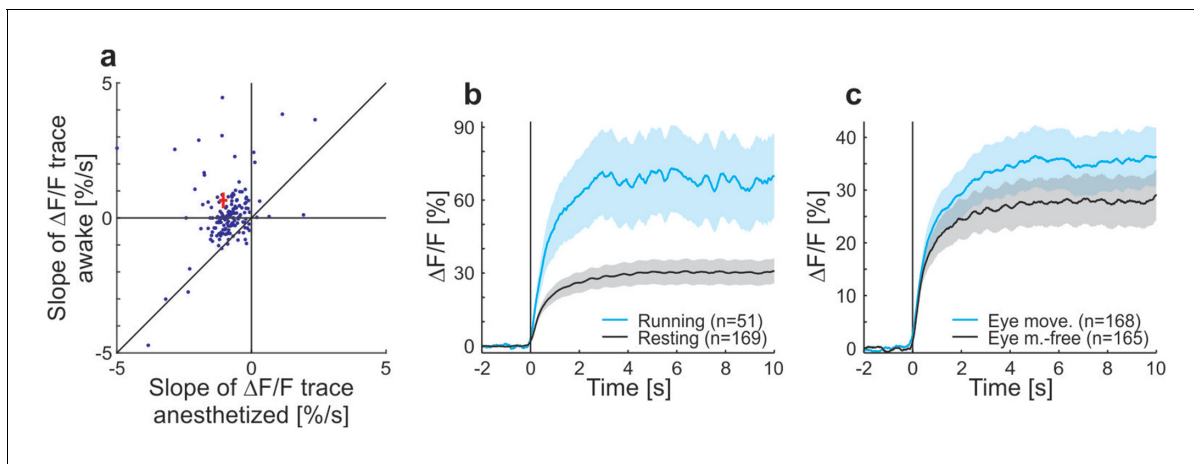


**Figure 1—figure supplement 3.** Contrast adaptation in anesthetized compared to awake mice and effects of running and eye movements on adaptation in awake mice. (a) Scatterplot showing slopes of adaptation of tuned putative excitatory cells recorded in anesthetized and awake mice (same cells as in **Figure 1c,d**; line fit to the data in time window 1–9.75 s). Seventeen cells not visible in the plot as they lie outside of the axis shown - 13 above and 4 below the diagonal. Red cross shows mean  $\pm$  SEM. (b) Averaged responses of tuned putative excitatory cells to a moving sinusoidal grating at 50% contrast presented for 10 s in awake running and resting mice. See also **Figure 1d**. Note that the number of cells for running (51 cells) is smaller than for the resting condition (169 cells) because not all cells were recorded in both conditions. Curves plotted as mean  $\pm$  SEM (shading). (c) Same as b but for trials with eye movements and eye movement-free trials.

DOI: [10.7554/eLife.21589.005](https://doi.org/10.7554/eLife.21589.005)

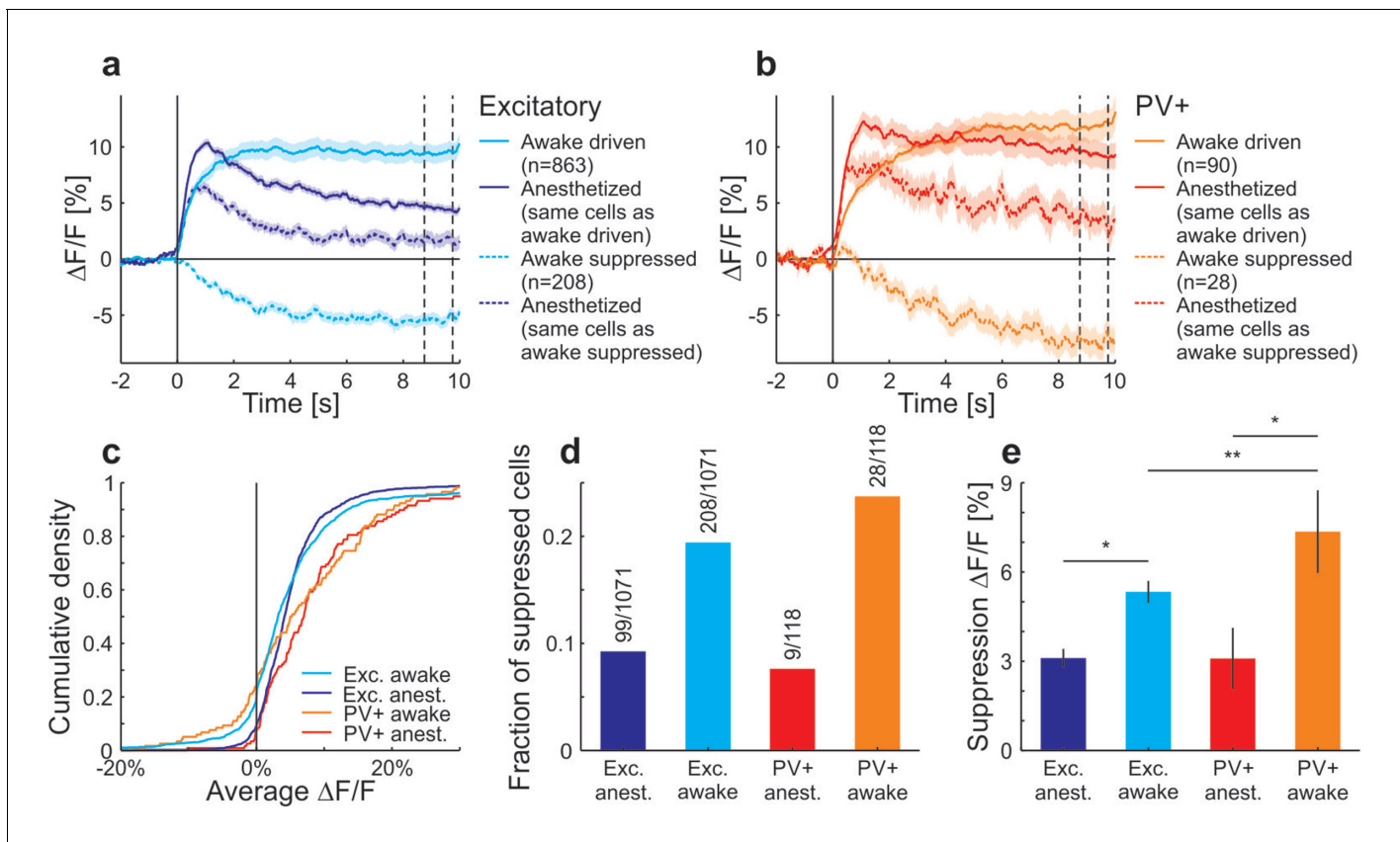


**Figure 1—figure supplement 4.** A large fraction of neurons in awake mice were suppressed during the stimulus and decreased their activity below baseline. The group of cells that were suppressed showed a positive average response under anesthesia. Of the putative excitatory cells, fewer cells showed a decrease compared to PV+ cells. Moreover, the magnitude of the decrease was larger for PV+ cells compared to putative excitatory cells. (a) All putative excitatory cells recorded in awake mice divided into groups which increase or decrease their activity in response to a moving sinusoidal grating at 50% contrast. The responses of the same groups of neurons are shown for the anesthetized mice. Note that the cells that are suppressed by the grating stimulation in awake mice are excited in anesthetized mice. The two vertical dotted lines indicate the time window which was used to compare the decrease in activity in c. Curves plotted as mean  $\pm$  SEM (shading). (b) Same as a but for PV+ cells. (c) Cumulative density of cells based on their average activity in response to the grating. (d) Fraction of putative excitatory and PV+ cells in awake and anesthetized mice with a negative average  $\Delta F/F$  (compared to baseline) in response to the grating. (e) The average decrease from baseline (of decreasing cells) in response to the grating (average of 8.75–9.75 s as indicated by the vertical dotted lines in a,b). Decreases are significantly larger in awake mice compared to anesthetized mice (putative excitatory awake: 208 cells; putative excitatory anesthetized: 99 cells;  $p=0.011$ ; PV+ awake: 28 cells; PV+ anesthetized: 9 cells;  $p=0.010$ ; Wilcoxon rank-sum). In awake mice, the decrease is significantly larger in PV+ compared to putative excitatory cells (putative excitatory: 208 cells; PV+: 28 cells;  $p=0.0038$ ; Wilcoxon rank-sum). \* $p<0.05$ ; \*\* $p<0.005$ .

DOI: [10.7554/eLife.21589.006](https://doi.org/10.7554/eLife.21589.006)



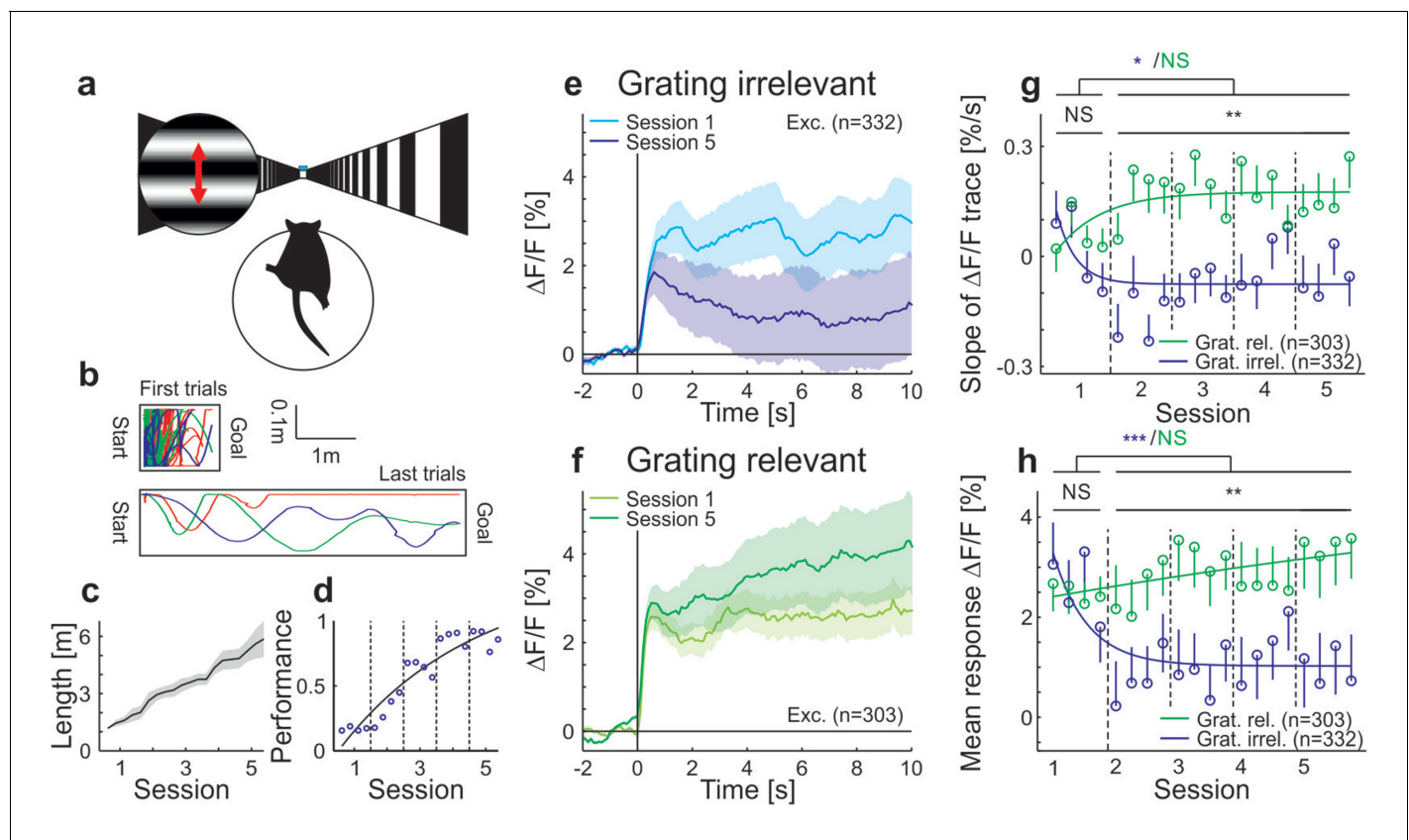


**Figure 2.** Adaptation is modulated by stimulus relevance in awake mice. **(a)** Schematic of the behavioral task. For the grating-irrelevant condition, movement of a virtual tunnel projected on a toroidal screen was coupled to the locomotion (rotation and running on a spherical treadmill) of the head-restrained mice (Dombek et al., 2007). Mice were trained to orient and run to the end of the tunnel for a water reward. We presented a horizontal sinusoidal moving grating in a circular probe patch centered on the retinotopic location of the recording site, interspersed with random intervals of gray (10–20 s; Video 1). **(b)** First and last paths of a sample mouse (four days apart). The colors show individual trials. **(c)** Task difficulty (length of the tunnel) was increased over learning to keep the number of rewards approximately constant. **(d)** Learning curve of an example mouse (solid line: exponential fit). The performance is quantified as the fraction of time spent running in the direction of the goal ( $\pm 25^\circ$ ). **(e)** Data from animals trained in the behavioral task under grating-irrelevant conditions. Traces show averaged calcium responses (GCaMP6f) (Chen et al., 2013) of tuned putative excitatory cells to a moving sinusoidal grating. Curves plotted as mean  $\pm$  SEM (shading). **(f)** Same as **e** but for animals exposed to the grating-relevant condition. For this condition, the visual stimulus on the screen was a replay of the visual flow from one of the mice in the grating-irrelevant group. To match the initial responses of the grating-relevant and the grating-irrelevant traces, ten percent of neurons were excluded from analysis (see Materials and methods). Note that this did not change the results. **(g)** Slopes of adaptation of the same cells as in **e** and **f** (line fit to the data in time window 1–10 s). In the grating-irrelevant condition, the slope significantly decreases from the first to the following sessions, as opposed to the grating-relevant condition (putative excitatory: 332 and 303 cells, respectively;  $p=0.017$  and  $p=0.28$ , respectively; Wilcoxon signed-rank). The slopes for the two conditions are similar during the first session, but significantly differ during later sessions (putative excitatory: 332 and 303 cells;  $p=0.84$  and  $p=0.0036$ , respectively; Wilcoxon rank-sum). The solid curves are exponential fits to the data. Error bars represent mean  $\pm$  SEM. **(h)** Same as **g** but for mean response to the grating. In the grating-irrelevant condition, the mean response significantly decreases from the first to the following sessions, as opposed to the grating-relevant condition (putative excitatory: 332 and 303 cells, respectively;  $p<10^{-4}$  and  $p=0.85$ , respectively; Wilcoxon signed-rank). The mean responses for the two conditions are similar during the first session, but significantly differ during later sessions (putative excitatory: 332 and 303 cells;  $p=0.61$  and  $p=0.0015$ , respectively; Wilcoxon rank-sum). NS, not significant; \* $p<0.05$ ; \*\* $p<0.005$ ; \*\*\* $p<0.0005$ .

DOI: 10.7554/eLife.21589.007

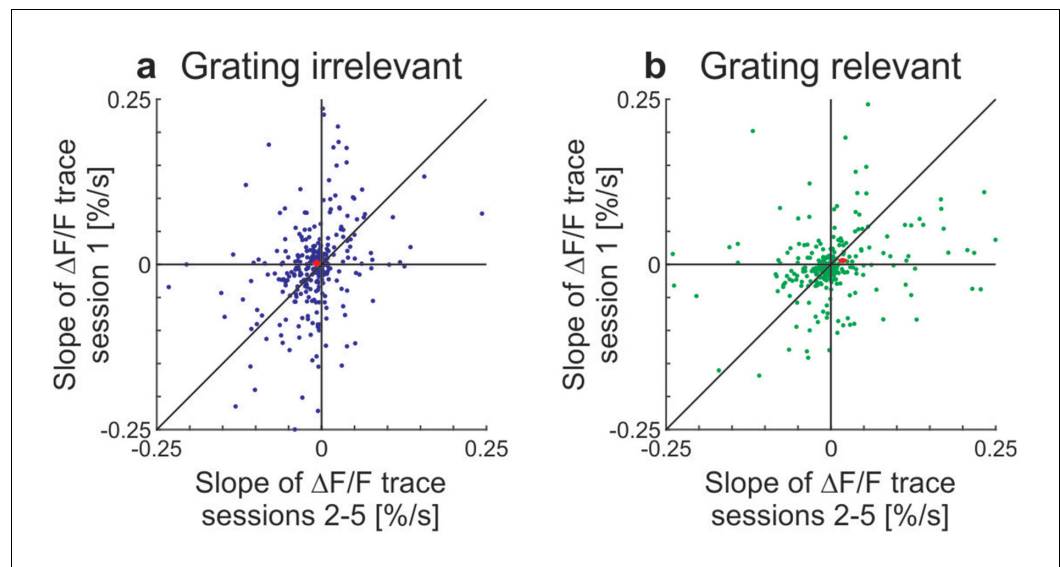


**Figure 2—figure supplement 1.** Scatterplots showing slopes of adaptation of the cells in training session one compared to the average slope in sessions 2–5 in awake mice (see also **Figure 2**; line fit to the data in time window 1–10 s). (a) Grating-irrelevant condition (same cells as in **Figure 2e,g**; 28 cells not visible in the plot as they lie outside of the axis shown, 16 above and 12 below the diagonal). Red cross shows mean  $\pm$  SEM. (b) Grating-relevant condition (same cells as in **Figure 2f,g**; 12 cells not visible in the plot as they lie outside of the axis shown, 3 above and 9 below the diagonal). Red cross shows mean  $\pm$  SEM.

DOI: [10.7554/eLife.21589.008](https://doi.org/10.7554/eLife.21589.008)

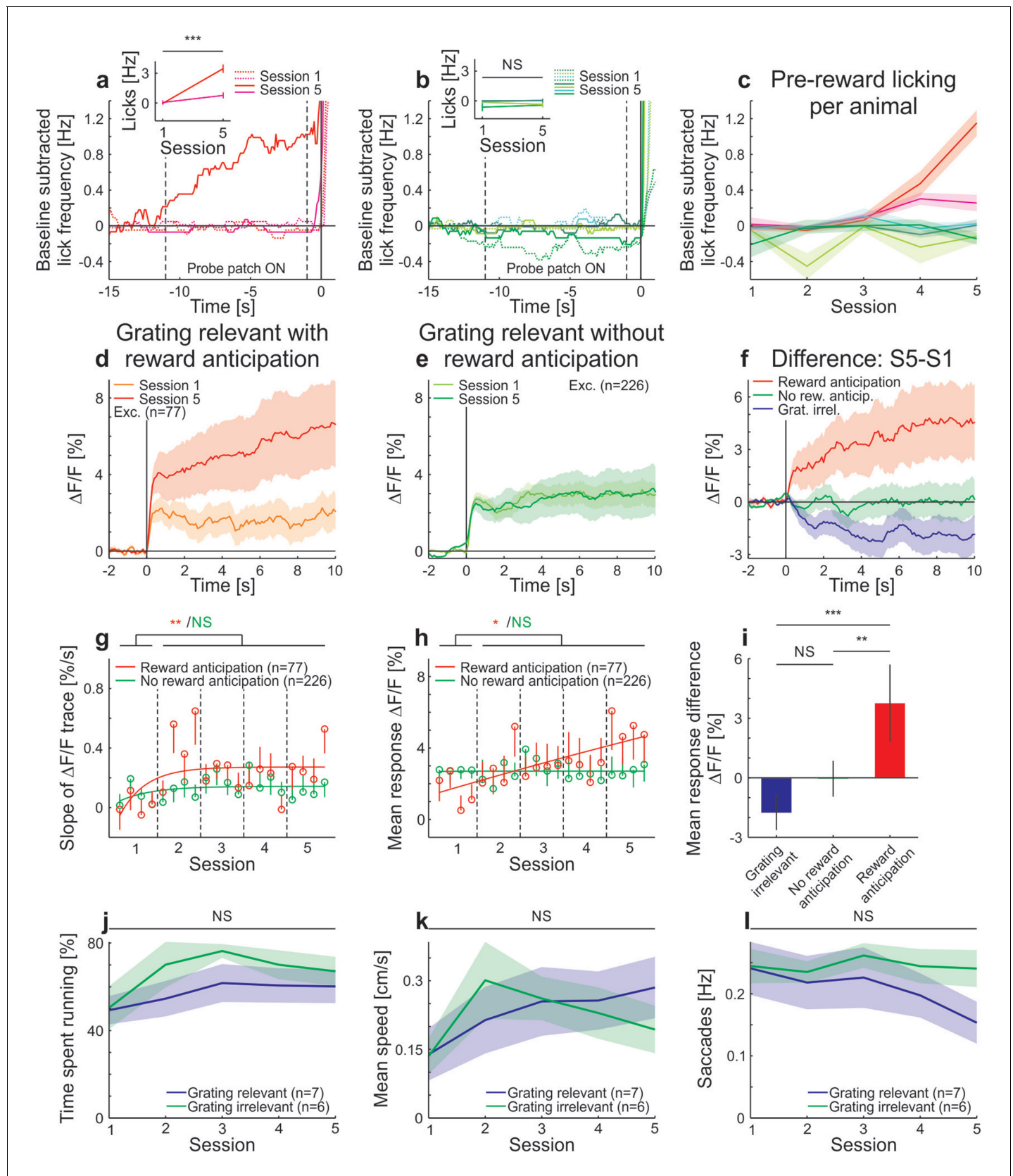


**Figure 2—figure supplement 2.** Licking, running, and eye-movement behavior in awake mice. (a–c) Lick frequency for grating-relevant condition. (a) Baseline subtracted lick frequency of the two animals showing a significant increase in anticipatory licking from session 1 (dotted colored lines) to session 5 (solid colored lines). The two vertical dotted lines indicate the stimulus presentation and the vertical solid line at 0 s indicates the water reward. Inset: Average anticipatory lick frequency (–0.5–0 s) is significantly higher in session five compared to session one in these two animals (session 1: 111 trials, session 5: 144 trials,  $p < 10^{-4}$  and session 1: 146 trials, session 5: 143 trials,  $p < 10^{-10}$ ; Wilcoxon rank-sum). (b) Same as a, but for the animals with no significant increase in anticipatory licking (session 1: 145 trials, session 5: 144 trials,  $p = 0.093$ ; session 1: 108 trials, session 5: 131 trials,  $p = 0.083$ ; session 1: 108 trials, session 5: 135 trials,  $p = 0.20$  and session 1: 144 trials, session 5: 135 trials,  $p = 0.49$ ; Wilcoxon rank-sum). (c) Average pre-reward lick frequency (–0.5–0s) for all animals over all sessions. (d) Averaged responses of tuned excitatory cells of the same animals as in a, to a moving sinusoidal grating (displayed in the probe patch) for sessions 1 and 5. Ten percent of the neurons were excluded to match the initial conditions of the grating-relevant traces to the grating-irrelevant traces (see Materials and methods for details). Note that this did not change the results. Curves plotted as mean  $\pm$  SEM (shading). (e) Averaged responses of tuned excitatory cells of the same animals as in b, to a moving sinusoidal grating (displayed in the probe patch) for sessions 1 and 5. Ten percent of the neurons were excluded to match the initial conditions of the grating-relevant traces to the grating-irrelevant traces (see Materials and methods for details). Note that this did not change the results. Curves plotted as mean  $\pm$  SEM (shading). (f) Traces show the differences in averaged responses of tuned excitatory cells between session 1 and 5 for the three conditions: grating-irrelevant; grating-relevant without anticipatory licking; and grating-relevant with anticipatory licking. (g) Slopes of adaptation of the same cells as in d and e are shown. For reward anticipating mice, the slope significantly increases from the first to the following sessions (putative excitatory: 77 cells;  $p = 0.0022$ ; Wilcoxon signed-rank). For the non-anticipating mice, the slope did not show any significant difference from the first to the following sessions (putative excitatory: 226 cells;  $p = 0.45$ ; Wilcoxon signed-rank). The trials of each session were divided into four quarters. The vertical dashed lines separate the individual sessions. The solid curve is an exponential fit to the data. Error bars represent mean  $\pm$  SEM. (h) Same as g but for mean response to the grating. For reward anticipating mice, the mean response significantly increases from the first to the following sessions (putative excitatory: 77 cells;  $p = 0.020$ ; Wilcoxon signed-rank). For the non-anticipating mice, the mean response did not show any significant change from the first to the following sessions (putative excitatory: 226 cells;  $p = 0.23$ ; Wilcoxon signed-rank). (i) Bar plot shows the mean response difference (session 5 – session 1) for the three traces in f. Reward anticipating mice have a significantly larger response difference compared to mice under grating-relevant condition (77 cells and 332 cells, respectively;  $p < 10^{-4}$ ; Wilcoxon rank-sum) or non-anticipating mice (77 cells and 226 cells, respectively;  $p = 9.0 \times 10^{-4}$ ; Wilcoxon rank-sum). There is no significant difference between grating-irrelevant and non-anticipating mice (332 cells and 226 cells, respectively;  $p = 0.13$ ; Wilcoxon rank-sum). (j) Proportion of time spent running over sessions for grating-irrelevant and grating-relevant conditions. The time spent running is not significantly different for the grating-irrelevant compared to the grating-relevant condition (7 and 6 mice; session 1:  $p = 0.84$ ; session 2:  $p = 0.18$ ; session 3:  $p = 0.53$ ; session 4:  $p = 0.45$ ; session 5:  $p = 0.23$ ; Wilcoxon rank-sum). Curves plotted as mean  $\pm$  SEM (shading). (k) Same as j, but for mean speed. The mean speed is not significantly different for the grating-irrelevant compared to the grating-relevant condition (7 and 6 mice; session 1:  $p = 0.84$ ; session 2:  $p = 0.45$ ; session 3:  $p = 0.95$ ; session 4:  $p = 0.84$ ; session 5:  $p = 0.29$ ; Wilcoxon rank-sum). Curves plotted as mean  $\pm$  SEM (shading). (l) Same as j but for saccade frequency. The saccade frequency is not significantly different for the grating-irrelevant compared to the grating-relevant condition (7 and 6 mice; session 1:  $p = 0.63$ ; session 2:  $p = 0.84$ ; session 3:  $p = 0.53$ ; session 4:  $p = 0.45$ ; session 5:  $p = 0.073$ ; Wilcoxon rank-sum). Curves plotted as mean  $\pm$  SEM (shading). NS, not significant; \* $p < 0.05$ ; \*\* $p < 0.005$ ; \*\*\* $p < 0.0005$ .

DOI: [10.7554/eLife.21589.009](https://doi.org/10.7554/eLife.21589.009)